THE EFFECT OF GAS RELEASE ON COLUMN SEPARATION*

Report No. 74-3

C. Kranenburg
Delft University of Technology
Department of Civil Engineering
Laboratory of Fluid Mechanics

* Apart from some modifications, the first four sections of this report also form part of a paper "Gas release during transient cavitation in pipes" published in the Journal of the Hydraulics Division, Proc. ASCE, Vol. 100, No. HY10, Oct., 1974.

CONTENTS

INTRODUCTION

The behaviour of a liquid at low pressures continues to be a subject of discussion as regards the water-hamer analysis of a pipeline transporting the liquid. Experiments on natural liquids have shown (9) that at pressures sufficiently less than the saturation pressure of dissolved gas, so-called cavitation nuclei grow to small gas bubbles as a result of gas diffusion. The lowest pressure that can be attained is equal to the vapour pressure of the liquid, or somewhat less because of the presence of surface tension. Further increase of the volume of the liquid-bubble mixture does not change the pressure but only increases the vapour content, a phenomenon known as cavitation of the liquid.

In a pipeline two types of transient cavitation can be distinguished. The void fraction (the ratio between the volume of vapour and gas, and total volume) depends on the magnitude of the velocity gradient in a pipe section in which cavitation occurs, and can increase to values comparable to unity for large velocity gradients, or can only attain values much less than unity for small velocity gradients owing to a friction gradient or a small inclination of the pipeline. The former type is known as column separation, generally displays a free-surface flow, and occurs locally in the pipeline ((1), (13) and (15)). The latter type, referred to as cavitating flow herein, is of the bubbly flow type, and can extend over distances comparable to the length of the pipeline ((7), (10), (5), (17) and (11)).

The examination of the phenomenon of water hammer together with transient cavitation is in an advanced state, but some doubts still exist as to secondary effects, such as the release of dissolved gas, on the maximum pressures and the duration of cavitation. Swaffield (15), for instance, consideres column separation behind a closing valve in a relatively short pipe, and observes a longer duration of the first column separation than predicted by classical methods without taking into account the influence of released gas. A similar result is obtained by Brown (3) for cavitation in a long pipeline following pump failure. In this case the computed maximum pressures are considerably less than the experimental values. Both authors obtain better agreement with observations by assuming that at discrete cavities a certain amount of dissolved gas is released from the liquid during low pressures. On the other hand, Baltzer (1), and Weyler, Streeter and Larsen (18) observe a shorter duration of the first column separation following sudden valve closure; subsequent pressures are lower than predicted. The results obtained by Dijkman and Vreugdenhil (5), and the writer (10) and (11)), showing that gas release causes damping of pressure waves following cavitating flow, point in the same direction.

The purpose of this report is to present some applications of a mathematical model, which describes the transient flow in pipelines, taking into account column separation and cavitating flow. It is shown that the aforementioned discrepancies between theory and experiments, and between observations by various authors can be explained by introducing the influence of gas release not only at column separations but also in the remaining part of the pipeline. Since the interpretation of the physical process and application of the mathematical model to cavitating flow have already been published ((7), (10) and (17)), emphasis is placed on the numerical methods adopted, and on application of the model to column separation. Additional information to these topics is given in (11).

OUTLINE OF THE MATHEMATICAL MODEL

The mathematical model is based on a one-dimensional approach to the flow of the liquid-vapour-gas mixture. Generally speaking, heat transfer processes related to the cavities are fast processes in comparison with the time scale of pressure changes ((6) and (11)). Therefore, the vapour pressure and gas temperature in the cavities can be assumed to be constant. The gravity term owing to the density gradient of the fluid along the pipeline is disregarded, so that in the model gravity waves do not occur. The resulting error in the pressures is of the order of magnitude of $\rho_l gD$ (in which ρ_l = liquid density, g = gravitational constant, and D = diameter of the pipe), which, in general, is small when compared with the water-hammer pressures. The momentum of the gas and vapour phases is disregarded with respect to the momentum of the liquid phase.

Conservation Laws.- Applying the law of conservation of mass to the liquid yields

$$\frac{\partial}{\partial t} \int_A (1-\alpha)\rho_l \, dA + \frac{\partial}{\partial x} \int_A (1-\alpha)\rho_l u \, dA = 0 \qquad (1)$$

in which α = local void fraction, i.e. dependent on the position in the cross-section, on coordinate x along the pipeline and on time t, u = liquid velocity, and A = area of cross-section of the pipe. The law of conservation of monentum, applied in the direction of the axis of the pipeline, yields

$$\frac{\partial}{\partial t} \int_A (1-\alpha)\rho_l u \, dA + \frac{\partial}{\partial x} \int_A (1-\alpha)\rho_l u^2 \, dA + \int_A \frac{\partial p}{\partial x} \, dA = \qquad (2)$$

$$= - \int_A (1-\alpha)\left(\rho_l g \sin\phi + \frac{\lambda}{2D} u\,|u|\right) dA$$

in which p = absolute pressure in the top of the cross-section of the pipe, ϕ = angle of inclination of the pipeline, and λ = friction parameter. Introducing the void-fraction

$$\bar{\alpha} = \int_A \alpha \, dA \tag{3}$$

and the usual equations of state of the liquid phase and the wall of a pipe with circular cross-section,

$$\frac{d\rho_l}{dp} = \frac{\rho_l}{K_l} \tag{4}$$

$$\frac{dA}{dp} = m \frac{A}{\frac{w}{D} E} \tag{5}$$

in which K_l = modulus of compressibility of the liquid, E = modulus of elasticity of pipe wall material, w = thickness of the wall of the pipe, and m = coefficient accounting for anchorage system of pipeline, and disregarding some minor contributions, changes Eqs. 1 and 2 to

$$\frac{\partial}{\partial t}(1-\bar{\alpha})\left(1+\frac{p}{\rho_l a_l^2}\right) + \frac{\partial}{\partial x}(1-\bar{\alpha})\left(1+\frac{p}{\rho_l a_l^2}\right)u = 0 \tag{6}$$

$$\frac{\partial}{\partial t}(1-\bar{\alpha})\left(1+\frac{p}{\rho_l a_l^2}\right)u + \frac{\partial}{\partial x}\left[(1-\bar{\alpha})\left(1+\frac{p}{\rho_l a_l^2}\right)u^2 + \frac{p}{\rho_l}\right] = -(1-\bar{\alpha})\left(g \sin\phi + \frac{\lambda}{2D} u\,|u|\right) \tag{7}$$

in which a_l = wave celerity in the absence of released gas or vapour,

$$\frac{1}{\rho_l a_l^2} = \frac{1}{K_l} + \frac{m}{\frac{w}{D} E} \tag{8}$$

Eqs. 6 and 7 are in the so-called conservation form, which is suitable for the numerical computation of wave propagation. Shock conditions, which are the equivalents of Eqs. 6 and 7 for discontinuities in velocity and pressure, are derived in the Appendix. They read

$$a_{sh}\,\Delta\left[(1-\bar{\alpha})\left(1+\frac{p}{\rho_l a_l^2}\right)\right] = \Delta\left[(1-\bar{\alpha})\left(1+\frac{p}{\rho_l a_l^2}\right)u\right] \tag{9}$$

$$a_{sh}\,\Delta\left[(1-\bar{\alpha})\left(1+\frac{p}{\rho_l a_l^2}\right)u\right]=\Delta\left[(1-\bar{\alpha})\left(1+\frac{p}{\rho_l a_l^2}\right)u^2+\frac{p}{\rho_l}\right] \qquad (10)$$

in which a_{sh} = shock-wave celerity, and Δ indicates the change in a variable when the shock wave is crossed. It is also shown in the Appendix, that at shock waves energy dissipation takes place.

Cavitating Flow.-Apart from column separation, the cavities will be present in the form of bubbles suspended in the liquid, which is connected with the small void fraction ($\bar{\alpha} << 1$). Adopting the ideal-gas law and disregarding surface tension yields for the dynamic equilibrium of a spherical bubble

$$(p-p_v)\,\frac{4}{3}\,\pi R^3 = N_b\,kT \qquad (11)$$

in which p_v = vapour pressure of the liquid, R = bubble radius, N_b = quantity of gas in the bubble, k = universal gas constant, and T = absolute temperature. Assuming a constant number, n_b, of bubbles (or cavitation nuclei) per running metre of the pipe and locally equal size of the bubbles, the average void-fraction becomes

$$\bar{\alpha} = \frac{n_b}{A}\,\frac{4}{3}\,\pi R^3 \qquad (12)$$

When the pressure is significantly higher than the vapour pressure, the bubble sizes, and hence the void fraction, can reduce so much that the free-gas content may be disregarded. In this case Eqs. 6 and 7 reduce to the usual water-hammer equations. Therefore, Eqs. 6 and 7 are applied in regions of the pipeline where cavitating flow occurs as well as in regions with higher pressures. The influence of gas content and surface tension on the wave celerity and the genesis of cavitation is discussed in (7), (10) and (11).

The quantity of gas, N_b, in a bubble is time dependent owing to the release or re-solution of gas. A general expression describing this process is

$$\frac{dN_b}{dt} = \gamma\,(p_s - p)\,\sqrt{\beta}\,F\left[R(\tau),\ \frac{dR(\tau)}{d\tau},\ U(\tau)\right] \qquad (13)$$

in which γ = proportionality constant in the relationship between gas pressure and equilibrium concentration of the dissolved gas, which relationship is known as Henry's law, p_s = saturation pressure of the liquid, β = diffusion coefficient τ = dummy variable in integration with respect to time ($\tau \leq t$), and U = velocity of the bubble with respect to the surrounding liquid. Function F, in which the history of the bubble is represented, can be determined from the solution of the dif-

fision equation for the dissolved gas (11). A useful approximation, which applies provided $|dR/dt| << U$ and $UR/\beta >> 1$, was given by Boussinesq (2), i.e.

$$F \simeq 4 R(t) \sqrt{2\pi U(t) R(t)} \tag{14}$$

Column Separation.-Since a column separation can be conceived of as a local phenomenon, the usual assumption is made that it is governed by the continuity equation only,

$$\frac{dV_c}{dt} = A (u_{c2} - u_{c1}) \tag{15}$$

in which V_c = volume of column separation, and $u_{c1,2}$ = liquid velocities on either side of the column separation. The ideal-gas law yields

$$(p_c - p_v) V_c = N_c kT \tag{16}$$

in which p_c = pressure at column separation, and N_c = quantity of released gas at column separation. Gas release or re-solution at the column separation is represented by

$$\frac{dN_c}{dt} = n_c \frac{dN_b}{dt} \tag{17}$$

in which n_c = number of bubbles which together form the column separation ($n_c \geq 1$), and dN_b/dt is given by Eq. 13, in which $p = p_c$.

NUMERICAL METHODS

Wave Equations,- The equations of continuity and momentum, Eqs. 6 and 7, together with the equations of state, Eqs. 11, 12 and 13, form a nonlinear hyperbolic system of second order. Such a system could, in principle, be solved using the method of integration along characteristics. This method, however, meets with considerable difficulties because of the pressure dependence of the wave celerity, which makes intersection of characteristics of the same kind possible. In simple cases the resulting discontinuities or shock waves can be fitted in the continuous solution, but in more general cases this method is hardly applicable ((7), (8)).

A second possibility as regards the solution of the wave equations is an approximation based on a finite-difference method. Since the problem is essen-

tially nonlinear owing to the marked pressure dependence of the celerity for pressures close to the vapour pressure, the finite-difference approximation adopted should contain numerical viscosity, which suppresses nonlineair instability and spreads a developing shock wave over a number of mesh points (12). Therefore, well-known finite-difference schemes like the leap-frog scheme and the impliciet scheme proposed by Streeter (14) are not applicable in this case. Finite-difference schemes which do contain numerical viscosity are, for instance, the Lax scheme and the Lax-Wendroff scheme, which emanate from the application of numerical methods to gas dynamics (12).

The continuity and momentum equations (Eqs. 6 and 7, are in conservation form

$$\frac{\partial q_{1i}}{\partial t} + \frac{\partial q_{2i}}{\partial x} = q_{3i} \tag{18}$$

in which q_{ji} ($j = 1,2,3$ and $i = 1,2$) are functions of the pressure, velocity and void fraction. The Lax scheme, applied to Eq. 18, yields (see Fig. 1)

$$q_{1i}\,(x + \Delta x,\ t + \Delta t) = \frac{1}{2}\left[q_{1i}\,(x + 2\,\Delta x,\ t) + q_{1i}\,(x,t)\right] + \tag{19}$$

$$- \frac{\Delta t}{2\Delta x}\left[q_{2i}\,(x + 2\Delta x,\ t) - q_{2i}\,(x,t)\right] + \frac{\Delta t}{2}\left[q_{3i}\,(x + 2\Delta x,t) + q_{3i}\,(x,t)\right]$$

in which Δx = mesh size, and Δt = time step. The numerical viscosity is introduced by the first term on the right-hand side of Eq. 19.

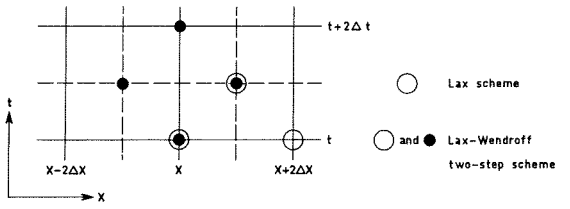

Fig. 1. Lax and Lax-Wendroff finite-difference schemes.

Unfortunately, the Lax scheme causes considerable damping of waves, owing to its first-order accuracy. This would lead to too low values for the maximum pressures. Second-order accuracy can be obtained by adding a second step to Eq. 19, according to (see Fig. 1)

$$q_{1i}\,(x,\ t+2\Delta t) = q_{1i}\,(x,t) - \frac{\Delta t}{\Delta x}\Big[q_{2i}\,(x+\Delta x,\ t+\Delta t) - q_{2i}\,(x-\Delta x,\ t+\Delta t)\Big] + \Delta t\Big[q_{3i}\,(x+\Delta x,\ t+\Delta t) + q_{3i}\,(x-\Delta x,\ t+\Delta t)\Big] \qquad (20)$$

Eqs. 19 and 20 together are known as the Lax-Wendroff two-step scheme. The numerical damping caused by this scheme is acceptable, provided a sufficient number of mesh points is chosen (11). The Lax-Wendroff scheme can be shown to be consistent with the differential equation, Eq. 18, and to be linearly stable, provided

$$\frac{\Delta t}{\Delta x} \leq \frac{1}{a_l + |u|} \qquad (21)$$

and

$$\Delta t < \frac{D}{\lambda |u|} \qquad (22)$$

Test runs carried out with the Lax-Wendroff scheme showed that his scheme yields satisfactory results in cases where the nonlinearity does not exeed certain bounds. However, in cases where the pressure dropped to vapour pressure, for instance, the essential nonlinearity of the problem caused oscillations, and instability of the computation. A possibility of suppressing this instability is to apply more numerical viscosity. On the other hand, as little viscosity as possible should be introduced, in order to avoid undesired wave damping. Therefore, numerical viscosity has been added by applying a smoothening operator in those mesh points in which a parameter, θ_i, characterizing the osillation in variable q_{1i} exceeds a prescribed value θ_r. The parameter θ_i is given by (see Fig. 2)

$$\theta_i\,(x,t) = \frac{\frac{1}{2}\,q_{1i}(x+2\Delta x,t) - q_{1i}(x,t) + \frac{1}{2}\,q_{1i}(x-2\Delta x,t)}{q_{ri}} \qquad (23)$$

in which q_{ri} = reference interval of variable $q_{1i}\,(x,t)$. The smoothened values $\bar{q}_{1i}$ of variable q_{1i} are obtained from

$$q_{1i}\,(x,t) = \begin{cases} q_{1i}\,(x,t) + \frac{1}{2}\,q_{ri}\,\theta_i\,(x,t), & |\theta_i| > \theta_r \\ q_{1i}\,(x,t), & |\theta_i| < \theta_r \end{cases} \qquad (24)$$

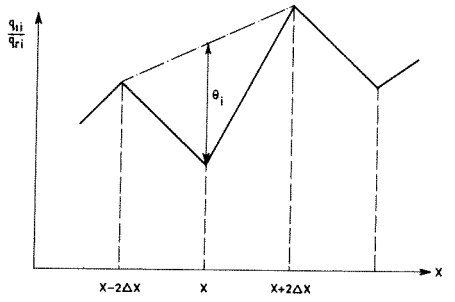

Fig. 2. Parameter θ_i in smoothening operator.

θ_r can be so chosen, that long waves (when compared with the mesh size) are only slightly influenced by the smoothening procedure (11). In the computations carried out the values θ_r = 0.01 and 0.05 were used. Vliegenthart (16) applied Eq. 23 in all mesh points (θ_r = 0).

Column Separation. - Column separation is explicitly taken into account at mesh points where it can be expected to occur. Secondary column separations are disregarded, and are implicitly treated by the cavitating flow approach. Integration of the equations for column separation, Eqs. 15 and 16, could be carried out by using a simple explicit finite-difference scheme. Analysing such a scheme shows, however, that for small amounts (N_c) of free gas, time steps are required which are considerably less than that given by Eq. 21. Instead, an integration method has been chosen in which the velocities u_{c1} and u_{c2} are eliminated by applying the compatibility equations for the characteristic directions following from Eqs. 6 and 7 ((14), (11)),

$$u_{c1} + \frac{1}{\rho_l a_1}(p_c - p_v) = B_1 \tag{25}$$

and

$$u_{c2} - \frac{1}{\rho_l a_2}(p_c - p_v) = B_2 \tag{26}$$

in which $a_{1,2}$ = pressure dependent (because of free-gas content) wave celerities in adjacent mesh points on either side of the column separation, and $B_{1,2}$ = approximately constant functions of computed variables in adjacent mesh points (Fig. 3). If the cavity is formed behind a closed valve, for instance, the quantities $1/a_1$ and B_1 in Eq. 25 (or $1/a_2$ and B_2 in Eq. 26) are put equal to zero.

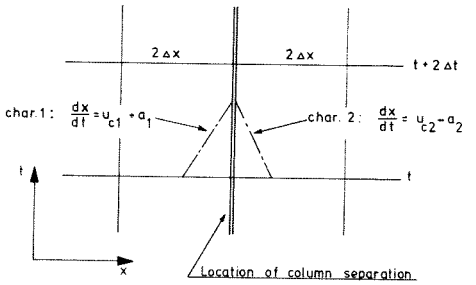

Fig. 3. Integration of the continuity equation for a cavity.

Eliminating velocities u_{c1} and u_{c2}, and pressure p_c from Eqs. 15,16,25 and 26, and integrating over a time step $2\Delta t$ (assuming N_c to be constant), yields

$$V_c(t+2\Delta t) = V_c(t) + 2\Delta t(B_1-B_2)A +$$

$$+\left(\frac{1}{a_1}+\frac{1}{a_2}\right)\frac{N_c kT}{\rho_l(B_1-B_2)}\ln\left[\frac{\left(\frac{1}{a_1}+\frac{1}{a_2}\right)N_c kT + \rho_l(B_1-B_2)V_c\,(t+2\Delta t)}{\left(\frac{1}{a_1}+\frac{1}{a_2}\right)N_c kT + \rho_l(B_1-B_2)V_c\,(t)}\right] \qquad (27)$$

The last term in this implicit finite-difference scheme can be seen as a correction to a simple first-order explicit scheme. Eq. 27 makes larger time steps possible without leading to instability. Moreover, this scheme always yields positive values of the cavity volume, $V_c(t + 2\Delta t)$. This property facilitates calculation of the collapse of a column separation. A small cavity is then left, owing to its free-gas content.

It was found from test computations that no smoothening should be carried out in grid points adjacent to a column separation.

Gas Release.- The equations decribing gas release or re-solution, Eqs. 13 and 17, were integrated at all points of the numerical mesh by using an explicit finite-difference technique (11).

APPLICATION TO BALTZER'S EXPERIMENTS

The simulation of column separation starting from classical water-hammer theory and the introduction of vapour pockets at suitable locations does not always yield satisfactory results. Swaffield (15) obtained the correct duration of column

separation, which was longer than predicted by standard methods, by assuming gas release at the column separation. Apparently, the shorter than predicted duration of column separation observed by Baltzer (1), for instance, requires a different explanation.

Using the methods developed in this report, some calculations were carried out for the model pipeline described by Baltzer. Column separation is generated in the author's pipeline (length = 136 m, diameter = 0.0254 m, a_l = 1360 m/s) by a sudden valve closure downstream. The resulting positive pressure wave is reflected upstream and causes column separation at the valve when it is reflected at that location. In his mathematical model, Baltzer assumes free-surface flow in the column separation cavity, and applied the usual water-hammer equations in the remaining part of the pipe. Fig. 4a shows a comparison, as regards the pressures at column separation, between Baltzer's theoretical results and the results of the method described herein, assuming no gas release. The mesh size was Δx = 2.72 m, the time step Δt = 0.002 s.

The agreement is satisfactory, indicating that the numerical method is reliable.

Gas release was assumed to occur in the computations related to Fig. 4b. The assumed numbers of bubbles per unit volume (n_b/A) were of the same order of magnitude as that obtained from previous experiments on cavitating flow ((10) and (11)), which amounted to about 10^5 bubbles/m^3. These experiments were also used to estimate the relative bubble velocity U from the growth of the bubbles during cavitation (10), or from the total amount of released gas (11). The estimates pointed to rather low values, i.e. less than some centimetres per second. In the present computations U = 0.01 m/s was assumed. Two values of the number of bubbles n_c which together form the column separation were considered (n_c = 1 and n_c = 1000). The saturation pressure was taken equal to the atmospheric pressure: $p_s = 10^5$ N/m^2. Furthermore, γkT = 0.017 and $\beta = 2 \times 10^{-9}$ m^2/s (air-water at 293 K) were assumed.

Computations No. 1 and 2 (in which twice the number of bubbles, n_b, of computation No. 1 was assumed) in Fig. 4b show that gas release in the cavitating flow region of the pipe causes a considerable decrease of the duration of the subsequent column separations and, connected with this, a decrease of the maximum pressures following column separation. This result can be explained as follows: gas release causes dilatation of the fluid column in the cavitating flow region, which dilatation can take place freely owing to the low pressure in the adjacent column separation cavity. Consequently, the volume of this cavity is less than that in the case without gas release, and the separation cavity collapses at an earlier instant. In the next section it is shown that a shock wave is then generated (the pressure rises in Fig. 4b), which starts to propagate in the up-

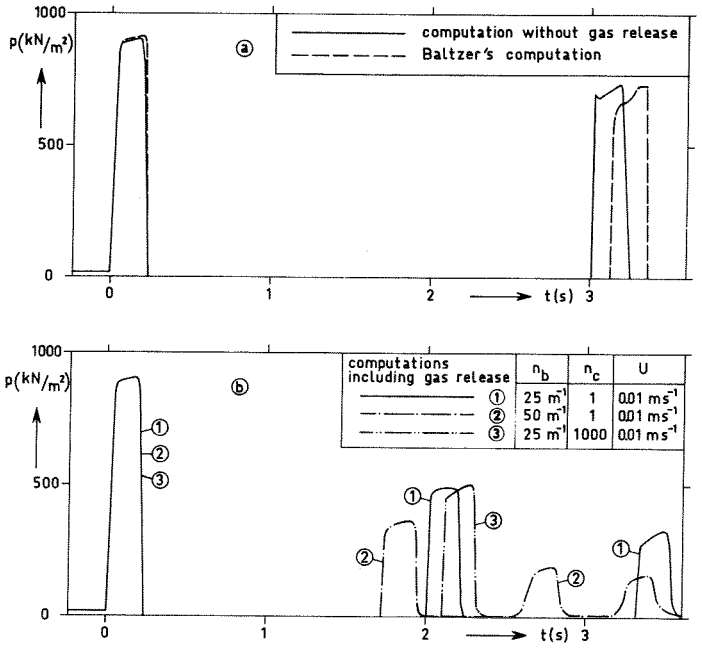

Fig. 4. Simulation of Baltzer's experiments and computation; pressures at column separation, a. disregarding gas release, b. including gas release.

stream direction. Owing to the small void fraction in the pipe, the shock celerity is only slightly less than the celerity a_1. Therefore the durations of the pressure peaks in Figs. 4a and 4b are the same. The maximum pressure following the first column separation is proportional to the liquid velocity at the instant of collapse. This velocity is less in Fig. 4b than in Fig. 4a, since less time is available for acceleration of the liquid column.

The above explanation of the damping phenomenon is based on the consideration of momentum. In the next section it is supplemented by examining the energy balance of the system.

If much gas is assumed to be released at the column separation (computation No. 3, n_c = 1000 instead of 1), the pressure at column separation remains higher than that in the cavitating flow region. Consequently, the fluid column shows less dilatation, and the column separation volume is less diminished. Therefore, the

instant of collapse is delayed (the third peak occurs at $t \approx 3.7$ s). Fig. 4b shows, however, that the cavitation process is not very sensitive to variations in the amount of released gas at column separation.

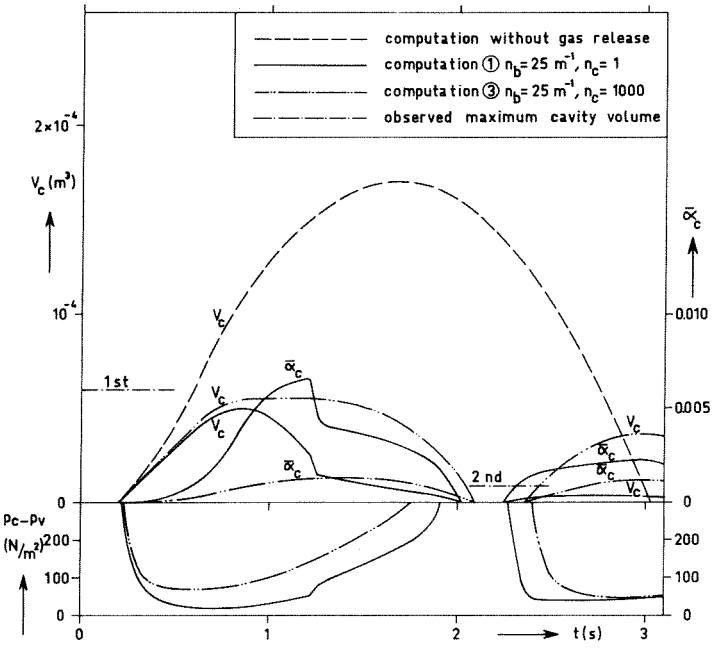

Fig. 5. Simulation of Baltzer's experiments: volume of cavity, pressure at column separation, and void fraction adjacent to column separation.

The preceding reasoning is further elucidated in Fig. 5, in which the volume of the column separation V_c, the void fraction $\bar{\alpha}_c$ in the adjacent part of the cavitating flow region, and the pressure p_c at column separation are shown as functions of time. It is seen that gas release decreases the volume of the separation, and that in computation No. 1 the void fraction $\bar{\alpha}_c$ is greater, the pressure p_c at separation is less, and the separation volume V_c is less than the corresponding variable in computation No. 3. Experimental values of the column separation volumes could be estimated by using Baltzer's wave height measurements. The maximum volumes are found to compare reasonably well with the theoretical values.

Fig. 6 shows a comparison between the pressures at column separation, as observed by Baltzer, and results of computation No. 1. Baltzer reports that his

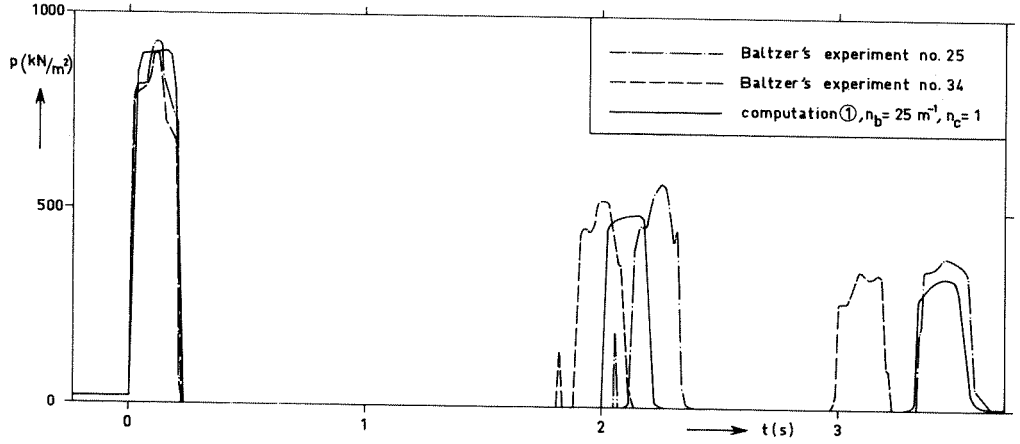

Fig. 6. Comparison between Baltzer's experimental results and computed results including the influence of gas release.

experiments No. 25 and No. 34 were carried out under the same laboratory conditions. The agreement achieved is good, which is, however, partly due to the choice of the gas-release parameters.

ENERGY BALANCE FOR HORIZONTAL PIPE

It may be surprising that the release of dissolved gas can account for a considerable damping of pressure peaks following column separation. The mechanism causing the damping should be part of the mathematical model discussed, but the numerical results do not reveal its origin. Even the question can be raised wether the damping could be caused by numerical damping effects coupled with the gas release. In principle this is not impossible, since the decrease of the wave celerity owing to gas release reduces the so-called Courant number, $a\Delta t/\Delta x$, of the numerical computation, which could increase the numerical damping ((11), (12)).

In order to make this point clear a hydrodynamic energy balance is set up for column separation in a pipe, closed at one end and connected to a constant-pressure reservoir ($p = p_r$) at the other end, see Fig. 7. For the sake of convenience a horizontal pipe is considered (Baltzer's pipe was an inclined one). The energy balance concerns the whole pipe, during the time interval between two successive pressure peaks (t_1-t_o, see Fig. 7). At $t = t_o$ and $t = t_1$ the liquid velocities are equal to zero, so that only elastic (potential) energy is present at these instants. In the time interval $t_o < t < t_1$ work is done at the constant-pressure end, elastic energy is converted into kinetic energy and vice versa, and energy is dissipated by shock waves and wall friction. The energy balance then expresses that the difference in elastic energies at $t = t_o$ and $t = t_1$, increased by the work at the constant-pressure end in the interval considered equals the dissipation.

Specifically, the following contributions to the energy balance are considered below:

I. elastic energy of the liquid and the wall of the pipe
II. elastic energy of the free gas
III. work done at the constant-pressure end ($x = l$) of the pipe
IV. dissipation caused by shock waves
V. dissipation caused by wall friction

Two cases are considered:

1. Influence of free gas only (terms I, II, III and IV)
2. Influence of wall friction only (terms I, III and V)

This separation facilitates the determination of the terms. Nevertheless it is not possible to accurately determine all terms in the energy balance; only approximate results are obtained.

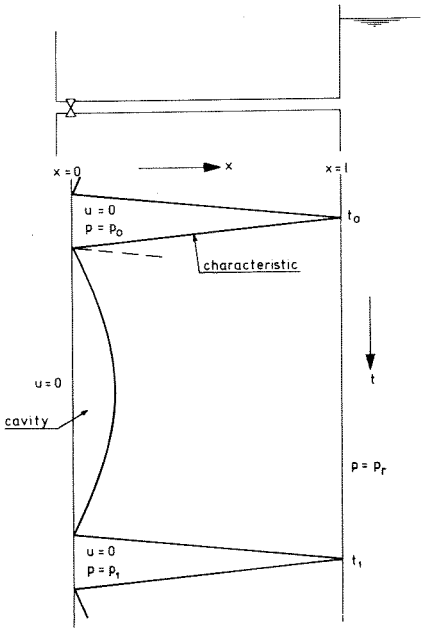

Fig. 7. Pipe and x,t-diagram.

1. Elastic Energy of the Liquid and the Wall of the Pipe. - The work done on a liquid column in an elastic pipe amounts to

$$W_l = - \int_{s_o}^{s_1} pA \, ds \tag{28}$$

in which $s_1 - s_o$ = increase in the length of the liquid column from $t = t_o$ to $t = t_1$. Variable s satisfies

$$\frac{ds}{dp} \simeq - \frac{l}{\rho_l a_l^2} \tag{29}$$

Consequently

$$W_l \simeq \frac{1}{2} V_l \frac{p_o^2 - p_1^2}{\rho_l a_l^2} \tag{30}$$

in which V_l = volume of the pipe (= lA), $p_o = p(t_o)$, and $p_1 = p(t_1)$.

II. Elastic Energy of the Free Gas. - Eq. 28 can also be applied in this case. The ideal gas law

$$(p - p_v)sA = \text{constant} = n_b N_b kTl \tag{31}$$

gives

$$\frac{ds}{dp} = - \frac{\mu l}{(p - p_v)^2} \tag{32}$$

in which $\mu = n_b N_b kT/A$. Eqs. 11 and 12 yield for this quantity

$$\mu = \bar{\alpha}_r (p_r - p_v) \tag{33}$$

in which subscript r refers to reservoir poressure.

The release of dissolved gas is taken into account by assuming that during the drop of the pressure from $p = p_o$ to a certain (low) cavitation pressure $p = p_*$ the amount of free gas remains constant ($\mu = \mu_o$), and that his amount increases to $\mu = \mu_1 > \mu_o$ during column separation, after which it is compressed from $p = p_*$ to $p = p_1$. An estimate of p_* is given later. Eqs. 28 and 32 then yield ($p_v \ll p_o$ and p_1)

$$\begin{aligned} W_{II} &\simeq V_l \left(\mu_o \int_{p_*}^{p_o} \frac{dp}{p - p_v} - \mu_1 \int_{p_*}^{p_1} \frac{dp}{p - p_v} \right) \\ &\simeq V_l \left(\mu_o \ln \frac{p_o}{p_* - p_v} - \mu_1 \ln \frac{p_1}{p_* - p_v} \right) \end{aligned} \tag{34}$$

III. Work Done at the Constant-Pressure End of the Pipe. - Since in this case $p = p_r$, Eq. 28 gives

$$W_{III} = - p_r A (s_1 - s_o) \tag{35}$$

$s_1 - s_o$ is determined by the elasticity of the liquid, the wall of the pipe, and the free gas (Eqs. 29 and 32). Hence

$$s_1 - s_o \simeq - \frac{l}{p_l a_l^2} (p_1 - p_o) + \frac{\mu_1}{p_1} l - \frac{\mu_o}{p_o} l \tag{36}$$

and

$$W_{III} \simeq - \rho_r V_1 \left(\frac{p_o - p_1}{\rho_1 a_1^2} + \frac{\mu_1}{p_1} - \frac{\mu_o}{p_o} \right) \qquad (37)$$

IV. Dissipation Caused by Shock Waves. - In the Appendix it is shown that the occurrence of shock waves is attended with dissipation of hydrodynamic energy. In the time interval $t_o < t < t_1$ two shock waves which attribute appreciably to the total dissipation, can be discerned.

At $t = t_o$ a rarefaction wave starts to travel from the constant-pressure end. This wave is positively reflected at the closed end, which causes column separation, and another rarefaction wave travelling backwards, see Fig. 8. In turn, this wave is negatively reflected at the constant-pressure end, so that a compression wave results. Since a low pressure is present in front of this wave, and consequently a low celerity, the wave will steepen rapidly and develop into a shock wave. The continued reflection of this wave causes alternately rarefaction and compression waves, but attenuation of these waves prevents the development of new shock waves (10).

The second shock wave is generated at the moment the column separation cavity is closed. The resulting sudden pressure rise, which then starts to propagate towards the reservoir, can be conveived of as a shock wave.

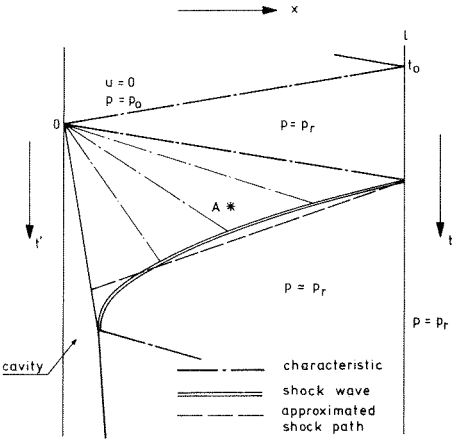

Fig. 8. x,t-diagram related to the first shock wave.

In order to determine the dissipation caused by the shock waves, the following simplifying assumptions are made:

- wall friction is absent (case 1 mentioned)
- the amount of free gas is constant, and is uniformly distributed along the pipe; since gas release at column separation was found to be relatively unimportant, it is not considered separately
- liquid velocities are negligible when compared with wave velocities.

The rarefaction wave starting at $x = 0$ at the instant the cavity opens, is given by (cf. the dam-break wave problem, (13))

$$\frac{x}{t'} = a(p)$$

in which t' = time, $t' = 0$ at the instant the cavity opens. Applying Eq. 22 from the Appendix,

$$\frac{1}{a^2} = \frac{1}{a_l^2} + \frac{\rho_l}{\mu_1}\bar{\alpha} = \left(\frac{t'}{x}\right)^2 \tag{38}$$

gives the void fraction $\bar{\alpha}$ as a function of time and position along the pipe. Eq. A21 then gives the pressure.

The fluid velocity, $u(p_v)$, behind the rarefraction wave, which is equal to the opening velocity of the cavity, is given by

$$u(p_v) = u(p_r) - \int_{p_v}^{p_r} \frac{dp}{\rho_l a(p)}$$

or, using Eqs. A21 and A22

$$u(p_v) = u(p_r) - \frac{1}{\rho_l}\int_{p_v}^{p_r} \sqrt{\frac{1}{a_l^2} + \frac{\rho_l \mu_1}{(p - p_v + \mu_1)^2}}\,dp \tag{39}$$

in which $u(p_r)$ = undisturbed fluid velocity in front of the wave. Restricting the analysis to cases where a vapour cavity really develops, i.e. to cases where

$$u(p_v) > 0$$

and integrating Eq. 39, yields

$$\sqrt{\frac{\mu_1}{\rho_l}}\left[\sqrt{\frac{(p_r - p_v)^2}{\mu_1 \rho_l a_l^2} + 1} - 1 + \ln\left\{2\frac{\rho_l a_l^2}{p_r - p_v}\left(\sqrt{\frac{(p_r - p_v)^2}{\mu_1 \rho_l a_l^2} + 1} - 1\right)\right\}\right] < u(pr) \tag{40}$$

which forms an upper limit for the free gas content μ_1. A numerical example: assuming $p_r - p_v = 10^5$ N/m^2 (atmospheric pressure), $\rho_l = 1000$ kg/m^3, $a_l = 1000$ m/s, and $u(p_r) = 1$ m/s, one obtains $\mu_1 < 11.7$ N/m^2, or $\bar{\alpha}_r < 1.17 \times 10^{-4}$ (Eq. 33).
The dissipation caused by the first-mentioned shock wave, which develops after reflection of the rarefaction wave, is estimated by applying Eq. A26. The total energy loss, $W_{IV\,1}$, related to this shock wave then is

$$W_{IV\,1} \simeq \frac{1}{2} A \int_{x(p_v)}^{l} (p_2 - p_v)\, \bar{\alpha}_{sh}\, dx \qquad (41)$$

in which $\bar{\alpha}_{sh}$ = void fraction just in front of the shock wave, $x(p_v)$ = value of x where $\bar{\alpha}_{sh} = 1$, and p_2 = pressure behind shock wave.
Assuming $p_2 \simeq p_r$, Eq. 41 simplifies to

$$W_{IV\,1} \simeq \frac{1}{2} A (p_r - p_v) \int_{x(p_v)}^{l} \bar{\alpha}_{sh}\, dx \qquad (42)$$

The shock path, $t' = t'_{sh}(x)$, follows from

$$\frac{dt'_{sh}}{dx} = -\frac{1}{a_{sh}} \quad \text{and} \quad t'_{sh}(l) = \frac{l}{a(p_r)} \qquad (43)$$

The shock celerity, a_{sh}, is given by Eq. A29. Further simplification is obtained by assuming a constant a_{sh} (denoted by a_o), which is, rather arbitrarily, put equal to the shock celerity at $x = l/2$, $t' = 3l/2a_l$ (point marked 'A' in Fig. 8). This gives, together with Eq. 38

$$\frac{1}{a_o^2} = \frac{1}{a_l^2} + \frac{\sqrt{8\,\rho_l \mu_1}}{a_l (p_r - p_v)}$$

On integration of Eqs. 43, time t'_{sh} is then found as a function of x, and Eq. 38 gives $\bar{\alpha}_{sh}$ as a function of x. Evaluating the integral in Eq. 42, and disregarding some minor contributions, yields for the energy loss related to the first shock wave

$$W_{IV\,1} \simeq p_r V_l \sqrt{\frac{\mu_1}{\rho_l a_o^2}} \left[\ln \left(2 \sqrt{\frac{\rho_l a_o^2}{\mu_1}} \right) - 2 \right] \qquad (44)$$

The pressure p_* appearing in Eq. 34 relates to the low pressures at which most of the free gas is released. It is estimated by averaging the lowest pressures occurring along the pipe, i.e.

$$\ln \frac{p_i}{p_* - p_v} = \frac{1}{l} \int_0^l \ln \frac{p_i}{p[x,\, t'_{sh}(x)]}\, dx \qquad (45)$$

in which subscript i = 0 or 1, and $p[x,t'_{sh}(x)]$ = pressure just in front of the shock wave. This pressure is determined by Eqs. 41, 42, 43 and Eq. A21. After some calculation, Eq. 45 yields

$$\ln \frac{p_i}{p_* - p_v} \simeq \ln \left(2 \frac{p_i}{a_o \sqrt{\rho_1 \mu_1}}\right) + \frac{1}{2} \tag{46}$$

The energy loss, $W_{lV\,2}$, caused by the second shock wave is given by an expression similar to Eq. 41,

$$W_{lV\,2} \simeq \frac{1}{2} A \int_o^l (p_1 - p_v)\, \bar{\alpha}_{sh}\, dx \tag{47}$$

in which p_1 = peak pressure following column separation. The void fraction $\bar{\alpha}_{sh}$ results from the pressure distribution in front of the pressure rise,

$$p \simeq p_v + \frac{x}{l} (p_r - p_v) \tag{48}$$

Applying Eq. 21 gives

$$\bar{\alpha}_{sh} \simeq \frac{\mu_1}{\mu_1 + \frac{x}{l} p_r} \tag{49}$$

so that Eq. 47 changes to

$$W_{lV\,2} \simeq \frac{1}{2} p_1 V_l \frac{\mu_1}{p_r} \ln \frac{p_r}{\mu_1} \tag{50}$$

V. Dissipation Caused by Wall Friction. - As an approximation, the dissipation by wall friction is estimated starting from the rigid-column assumption during separation. The work done on the wall by friction is then given by

$$W_V = \int_{t_o}^{t_1} \pi D l \tau u \, dt \tag{51}$$

in which τ = wall shear stress,

$$\tau = \frac{\lambda}{8} \rho_l \, u|u| \tag{52}$$

in which contributions caused by the unsteadiness of the flow are disregarded.

Assuming a linear velocity course from $u = u_o$ to $u = -u_o$ yields

$$\int_{t_o+l/a_l}^{t_1-l/a_l} u^2|u|dt = \frac{u_o^3}{4}\left(t_1 - t_o - \frac{2l}{a_l}\right) \tag{53}$$

Rigid-column theory gives: $du/dt \simeq -(p_r - p_v)/\rho_l l$, or

$$t_1 - t_o - \frac{2l}{a_l} \simeq 2u_o \frac{\rho_l l}{p_r - p_v} \tag{54}$$

Substituting these equations into Eq. 51 yields ($p_v << p_r$)

$$W_V \simeq \frac{\lambda}{16}\ \pi D l^2 \frac{\rho_l^2 u_o^4}{p_r} = \frac{\lambda}{4}\frac{l}{D} V_l \frac{\rho_l^2 u_o^4}{p_r} \tag{55}$$

Since

$$\frac{p_1 - p_r}{\rho_l a_l} < u_o < \frac{p_o - p_r}{\rho_l a_l}$$

the energy loss caused by wall friction is approximated by

$$W_V \simeq \frac{\lambda}{4}\frac{l}{D} V_l \frac{\rho_l^2}{p_r} \frac{1}{2}\left[\left(\frac{p_1 - p_r}{\rho_l a_l}\right)^4 + \left(\frac{p_o - p_r}{\rho_l a_l}\right)^4\right] \tag{56}$$

Eq. 54 is replaced by

$$t_1 - t_o \simeq \frac{\rho_l l}{p_r}\left(\frac{p_1 - p_r}{\rho_l a_l} + \frac{p_o - p_r}{\rho_l a_l}\right) + \frac{2l}{a_l} = \frac{l}{a_l}\frac{p_1 + p_o}{p_r} \tag{57}$$

<u>The Energy Balance</u>. - The energy balance reads in the case where only the influence of free gas is considered

$$W_I + W_{II} + W_{III} = W_{IV\,1} + W_{IV\,2} \tag{58}$$

In the case where only wall friction is considered, terms $W_{IV\,1} + W_{IV\,2}$ must be replaced by W_V.

Substituting the expressions obtained for the contributions to the energy balance yields an equation in which p_1 is the only unknown, provided the amounts of free gas, represented by μ_o and μ_1, are known.

Comparing the orders of magnitude of the terms in Eq. 58, it is found that generally the free-gas terms (those containing μ on the left-hand side, $\mu < 10$ N/m^2 in most practical cases) are small with respect to those on the right-hand side. This means that usually the damping effect of free gas is caused mainly by dissipation at shock waves, and that changes in elastic energy (W_{II}) and storage capacity (part of W_{III}) of the free gas are of minor importance. This also explains the relatively small influence of gas release at the column separation cavity. Furthermore, the damping caused by wall friction turns out to predominate at high pressures p_o and p_1 (large velocities), whereas at lower pressures the damping caused by shock waves is more important.

After the peak pressure p_1 has been determined from Eq. 58, this pressure can be seen as a starting value of a next column separation. Replacing in Eq. 58 p_o by p_1, and adjusting μ-values, makes the computation of a following peak pressure possible. Thus a complete sequence of pressure peaks can be determined.

An Example. - Fig. 9 shows some results obtained from the energy balance, Eq. 58. The assumed data of the pipe are

length	200 m
diameter	0.10 m
λ	0 or 0.02
a_l	1000 m/s
ρ_l	1000 kg/m^3
$p_r - p_v$	10^5 N/m^2 (atmospheric pressure)

The magnitude of the first pressure peak is 6×10^5 N/m^2 in all cases. The gas release parameters chosen are those of the preceding section. The grid size, Δx, in the numerical computations, the results of which are also shown in Fig. 9, was 4.00 m, the time step $t = 0.004$ s.

Fig. 9a shows a comparison between the theoretical pressure peaks and those computed numerically in the case where wall friction and gas release are disregarded. Numerical damping of any significance is not found.

Gas release is considered in Fig. 9b. The quantities of released gas appearing in the energy balance were adopted from the numerical computation concerned, i.e. $\mu_o = 0.003$, $\mu_1 = 0.4$, $\mu_2 = 0.75$ N/m^2. Although the agreement between energy balance and numerical computation is not complete, it can be concluded that the damping found in numerical computations including gas release has a physical origin, viz. dissipation caused by shock waves. Apparently, the contribution of numerical damping is small.

In Fig. 9c the results of the energy balance point to a weak damping in the case where only wall friction is assumed to occur.

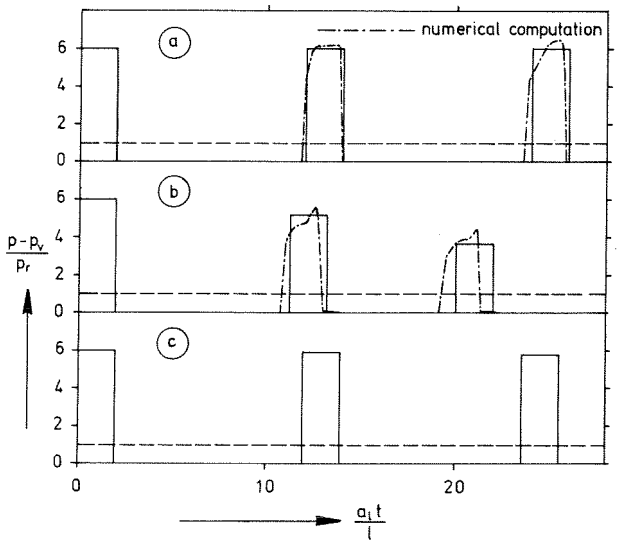

Fig. 9. Theoretical and computed damping of pressure peaks following column separation, a. no wall friction, no gas release, b. damping caused by gas release only, c. by wall friction only.

SUMMARY AND CONCLUSIONS

A mathematical model has been considered in which the influence of gas release on transient cavitating flow and column separation in pipelines is taken into account. A reliable numerical method has been developed for the computation of the wave propagation and cavitation phenomena following pump failure, valve closure, etc. Good agreement has been obtained with available experimental results concerning column separation.

Including gas release in the theory has no great influence in cases where only cavitating flow occurs, whereas the influence is considerable in cases where column separation together with cavitating flow occurs. Gas release in the cavitating flow region adjacent to a column separation cavity, which region will occur if the waves are steep (e.g., sudden valve closure), diminishes the duration of the subsequent column separations and the maximum pressures following column separation. The related energy loss can be attributed to dissipation caused by shock waves pro-

pagating in the bubble mixture. Gas release at the separation cavity has a different effect: the duration of column separation increases, and the pressures increase slight The former process is sensitive to the amount of gas released, whereas the latter is not.

If the valve closes, or the pump decelerates, slowly with respect to the wave travel time of a disturbance in the pipeline, the liquid column will behave as a rigid column during the first column separation, and no cavitating flow region will be generated. This means that gas release then takes place mainly at the column separation, so that the duration of column separation increases somewhat, and no additional damping (besides damping caused by friction) of the pressure peaks following separation is found. Swaffield (15) considered such a case. The more favorable situation in which this damping does take place, will occur if the valve closure or pump shut down is relatively fast, like, e.g., in the experiment carried out by Baltzer (1).

Since gas release depends on a number of parameters about which little is known (e.g., numbers of bubbles n_b and n_c, and relative bubble velocities), the quantitative prediction of the amount of gas being released in an arbitrary case, and its influence on the maximum pressures following column separation, requires further experimentation, probably on prototype scale.

APPENDIX

Shock Waves. - Before considering shock waves, some attention is devoted to continuous waves. The laws of conservation of mass and momentum for one-dimensional waves in an isothermal fluid are

$$\frac{\partial \rho_f}{\partial t} + \frac{\partial}{\partial x}(\rho_f u) = P \tag{A1}$$

and

$$\frac{\partial}{\partial t}(\rho_f u) + \frac{\partial}{\partial x}(\rho_f u^2 + p) = Q \tag{A2}$$

in which ρ_f = density of the fluid, P = production of mass, and Q = production of momentum. As regards the equation of state, it is assumed that the density depends on the pressure only,

$$\rho_f = \rho_f(p) \tag{A3}$$

The equation of motion, obtained by multiplying Eq. A1 by u and subtracting from Eq. A2, can be written

$$\frac{\partial u}{\partial t} + \frac{\partial}{\partial x}\left[\frac{1}{2}u^2 + \int^{p} \frac{dp'}{\rho_f(p')}\right] = \frac{1}{\rho_f}(Q - Pu) \tag{A4}$$

The characteristic directions, which represent the velocity of propagation of a small disturbance, are given by

$$\frac{dx}{dt} = u \pm \sqrt{\frac{dp}{d\rho_f}} = u \pm a \tag{A5}$$

The compatibility conditions along the characteristics are

$$\frac{1}{a}\frac{dp}{dt} \pm \rho_f \frac{du}{dt} = (a \mp u)P \pm Q \tag{A6}$$

Next, discontinuous waves or shock waves propagating in the same fluid are considered. A possible change in temperature of the fluid crossing the shock wave is assumed to be so small, that its influence on the fluid properties may be disregarded.

The derivation of shock conditions is simplified by attaching the coordinate system to the shock wave, so that a steady-state situation results. Therefore, a new fluid velocity is introduced according to

$$v = a_{sh} - u \tag{A7}$$

The law of conservation of mass then gives (Fig. A1)

$$\rho_{f2}\, v_2 - \rho_{f1}\, v_1 = P\, \delta x \tag{A8}$$

in which subscripts 1 and 2 refer to conditions in front of and behind the shock wave, respectively. Since the shock is conceived of as a discontinuity, the width δx of the region considered can be taken as infinitesimal, so that production terms, in this case $P\, \delta x$, vanish. Eq. A8 then changes to

$$\rho_{f2}\, v_2 - \rho_{f1}\, v_1 = 0 \tag{A9}$$

The law of conservation of momentum gives, again omitting the production term

$$\left[\rho_{f2}\, v_2^2 + p_2\right] - \left[\rho_{f1}\, v_1^2 + p_1\right] = 0 \tag{A10}$$

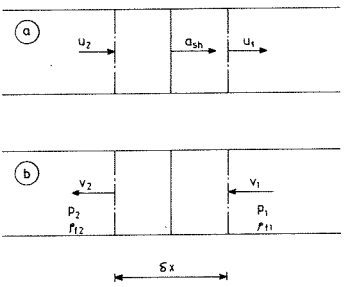

Fig. A1. Notation for shock wave, a. fixed coordinate system, b. coordinate system attached to shock wave.

The loss, W^*_{sh}, of hydrodynamical energy per unit mass crossing the shock wave follows from an energy balance,

$$\rho_{f2}\, v_2\, W^*_{sh} + \left[\frac{1}{2}\rho_{f2}\, v_2^3 + p_2\, v_2 - \rho_{f2}\, v_2 \int^{p_2} p'\, d\left(\frac{1}{\rho_f}\right)\right] +$$

$$- \left[\frac{1}{2}\rho_{f1}\, v_1^3 + p_1\, v_1 - \rho_{f1}\, v_1 \int^{p_1} p'\, d\left(\frac{1}{\rho_f}\right)\right] = 0$$

The first terms in brackets represent the transport of kinetic energy, the second the work done by the pressure, and the third the transport of elastic energy (elastic energy $= -\int p'ds$; considering a unit mass gives $s\rho_f = 1$, and $ds = d(1/\rho_f)$). Integrating the latter terms by parts, and using Eq. A9, yields

$$W^*_{sh} + \left[\frac{1}{2} v_2^2 + \int^{p_2} \frac{dp'}{\rho_f(p')}\right] - \left[\frac{1}{2} v_1^2 + \int^{p_1} \frac{dp'}{\rho_f(p')}\right] = 0 \qquad \text{(A11)}$$

Eqs. A9, A10 and A11 are the equivalents for discontinuous waves of Eqs. A1, A2 A4 for continuous waves. However, in Eq. A11 the dissipation term W^*_{sh} had to be introduced in order to avoid incompatibility of the equations. Eqs. A9 and A10 give

$$v_1^2 = \frac{\rho_{f2}}{\rho_{f1}} \frac{p_2 - p_1}{\rho_{f2} - \rho_{f1}} \qquad \text{and} \qquad v_2^2 = \frac{\rho_{f1}}{\rho_{f2}} \frac{p_2 - p_1}{\rho_{f2} - \rho_{f1}} \qquad \text{(A12)}$$

Substituting these results into Eq. A11 gives for the energy loss

$$W^*_{sh} = -\int_{p_1}^{p_2} \frac{dp'}{\rho_f(p')} + \frac{1}{2}\left(\frac{1}{\rho_{f1}} + \frac{1}{\rho_{f2}}\right)(p_2 - p_1) \qquad \text{(A13)}$$

The last term in this equation can be seen as an approximation of the integral according to the trapezium rule. Consequently, W^*_{sh} behaves as $(p_2-p_1)^3$ when p_2-p_1 tends to zero. This result shows that, apart from possible contributions of production terms, there is no energy loss in the case of continuous waves. If the wave is discontinuous, however, in general dissipation does take place.

Since any change in the hydrodynamical energy of the fluid crossing a shock wave must be a decrease (Second Law of thermodynamics), the condition

$$W^*_{sh} > 0 \qquad \text{(A14)}$$

must be satisfied. From Eq. A13 it then follows that the shock is a compression shock ($p_2 > p_1$) if

$$\frac{d^2}{dp^2}\left(\frac{1}{\rho_f}\right) > 0 \qquad \text{or, using Eq. A5,} \quad \frac{1}{\rho_f a} + \frac{da}{dp} > 0 \qquad \text{(A15)}$$

whereas it is a rarefaction shock ($p_2 < p_1$) if

$$\frac{d^2}{dp^2}\left(\frac{1}{\rho_f}\right) < 0 \qquad \text{or} \qquad \frac{1}{\rho_f a} + \frac{da}{dp} < 0 \tag{A16}$$

Disregarding production terms in Eq. A6, the compatibility condition along a characteristic in negative x-direction is $du/dp \simeq 1/\rho_f a$, so that along this characteristic

$$\frac{1}{\rho_f a} + \frac{da}{dp} \simeq \frac{d}{dp}(u + a) \tag{A17}$$

According to Eq. A5 the celerity of a small disturbance in positive x-direction is equal to $(u + a)$. In view of Eq. 17, condition A15 therefore also expresses that a compression wave steepens, and a rarefaction wave flattens, during its propagation. Consequently, only a compression wave can then develop into a shock wave. Condition A16 expresses the same for a rarefaction wave. Thus it is found that the energy condition, Eq. A14, is equivalent with the condition for the formation of a shock wave.

The celerity of a shock wave is found from Eqs. A7 and A12,

$$a_{sh} = u_1 + \sqrt{\frac{\rho_{f2}}{\rho_{f1}} \frac{p_2 - p_1}{\rho_{f2} - \rho_{f1}}} = u_2 + \sqrt{\frac{\rho_{f1}}{\rho_{f2}} \frac{p_2 - p_2}{\rho_{f2} - \rho_{f1}}} \tag{A18}$$

When $p_2 - p_1$ tends to zero (and consequently $u_2 - u_1$ and $\rho_{f2} - \rho_{f1}$), the celerity of infinitesimal waves, given by Eq. A5, is found again.

Application to the Bubble Mixture. - Comparing Eqs. 6 and A1, and Eqs. 7 and A2 shows that in this case

$$\rho_f = \rho_l \left(1 + \frac{p}{\rho_l a_l^2}\right)(1 - \bar{\alpha}) \tag{A19}$$

in which ρ_l is the (constant) liquid density at zero pressure. In Eq. A19 the density ρ_g of the gas is disregarded, which is justified provided

$$\bar{\alpha}\,\rho_g << (1 - \bar{\alpha})\,\rho_l \tag{A20}$$

Assuming a constant amount of free gas per unit mass of the fluid, the relation between the void fraction, $\bar{\alpha}$, and pressure is given by

$$\bar{\alpha} = \frac{\mu}{p - p_v + \mu} \tag{A21}$$

which reduces to Eqs. 11 and 12 if $\bar{\alpha} \ll 1$. This somewhat restricting assumption is not made here.

The celerity of a small disturbance, resulting from Eqs. A5, A19 and A21 is given by

$$\frac{1}{\rho_l a^2} \simeq \frac{1}{\rho_l a_l^2} + \frac{\bar{\alpha}^2}{\mu} \tag{A22}$$

The energy loss (Eq. A13) becomes

$$W^*_{sh} = - \int_{p_1}^{p_2} \frac{p - p_v + \mu}{p - p_v} \frac{dp}{\rho_l + \frac{p}{a_l^2}} + \\ + \frac{1}{2} \left[\frac{p_1 - p_v + \mu}{p_1 - p_v} \frac{1}{\rho_l + \frac{p_1}{a_l^2}} + \frac{p_2 - p_v + \mu}{p_2 - p_v} \frac{1}{\rho_l + \frac{p_2}{a_l^2}} \right] \tag{A23}$$

which, after some calculation, changes to

$$W^*_{sh} \simeq \frac{\mu}{\rho_l} \left[\frac{1}{2} \frac{p_2 - p_v}{p_1 - p_v} - \frac{1}{2} \frac{p_1 - p_v}{p_2 - p_v} - \ln \frac{p_2 - p_v}{p_1 - p_v} \right] + \\ + \frac{1}{6} a_l^2 \left[\frac{p_2 - p_1}{\rho_l a_l^2} \right]^3 \tag{A24}$$

which shows that only compression shocks ($p_2 > p_1$) are possible in this case. The last term in Eq. A24 does not vanish when the free-gas content, μ, tends to zero. It represents the theoretical possibility of shock formation caused by convective effects, and is completely negligible. The remaining expression is essentially that derived by Campbell and Pitcher (4) for the entropy increase (multiplied by temperature) across a shock wave. These authors also show that the increase in temperature of a mass of fluid crossing a shock wave is negligibly small.

In cases where $p_1 \ll p_2$ the energy loss becomes large, and can then be approximated by

$$W^*_{sh} \simeq \frac{1}{2} \frac{\mu}{\rho_l} \frac{p_2 - p_v}{p_1 - p_v} \tag{A25}$$

The volume of the unit mass is equal to $1/(1 - \bar{\alpha}_1)\rho_l$ in front of the shock. The energy loss W'_{sh} per unit volume of the fluid in front of the shock then amounts to

(see Eq. A21)

$$W'_{sh} \simeq \frac{1}{2} \bar{\alpha}_1 \, (p_2 - p_v) \tag{A26}$$

Eqs. A18, A19 and A21 give for the shock celerity a_{sh}

$$\frac{1}{\rho_l (a_{sh} - u_1)^2} \simeq \left(1 + \frac{p_2 - p_1}{\rho_l a_l^2}\right)^{-1} \frac{1 - \bar{\alpha}_1}{1 - \bar{\alpha}_2} \left(\frac{1}{\rho_l a_l^2} + \frac{\bar{\alpha}_1 \bar{\alpha}_2}{\mu}\right) \tag{A27}$$

and

$$\frac{1}{\rho_l (a_{sh} - u_2)^2} \simeq \left(1 + \frac{p_2 - p_1}{\rho_l a_l^2}\right) \frac{1 - \bar{\alpha}_2}{1 - \bar{\alpha}_1} \left(\frac{1}{\rho_l a_l^2} + \frac{\bar{\alpha}_1 \bar{\alpha}_2}{\mu}\right) \tag{A28}$$

For small void fractions and $(p_2 - p_1) \ll \rho_l a_l^2$ these expressions can be approximated by

$$\frac{1}{\rho_l (a_{sh} - u_1)^2} \simeq \frac{1}{\rho_l (a_{sh} - u_2)^2} \simeq \frac{1}{\rho_l a_l^2} + \frac{\bar{\alpha}_1 \bar{\alpha}_2}{\mu} \tag{A29}$$

Eqs. A6 and A8 yield

$$(\rho_{f2} - \rho_{f1}) a_{sh} = \rho_{f2} u_2 - \rho_{f1} u_1 \tag{A30}$$

Using this result, Eqs. A6 and A9 give

$$(\rho_{f2} u_2 - \rho_{f1} u_1) a_{sh} = (\rho_{f2} u_2^2 + p_2) - (\rho_{f1} u_1^2 + p_1) \tag{A31}$$

Eqs. 9 and 10 are obtained by substituting Eq. A19 into the latter two relationships.

Example of Energy Loss Caused by a Shock Wave.- In order to illustrate the results obtained in the preceding sections, the following situation is considered: a horizontal pipe containing liquid and vapour at rest is closed at one end ($x = 0$) and connected to a constant-pressure reservoir at the other end ($x = l$, $p = p_r$); the valve at $x = l$ is closed, see Fig. A2. At $t = 0$ this valve is opened instantaneously. As regards the position of the vapour void two cases are considered,

a. the vapour is concentrated in a single cavity at $x = 0$ (Fig. A2a)

b. the same volume of vapour is uniformly distributed along the pipe (Fig. A2b)

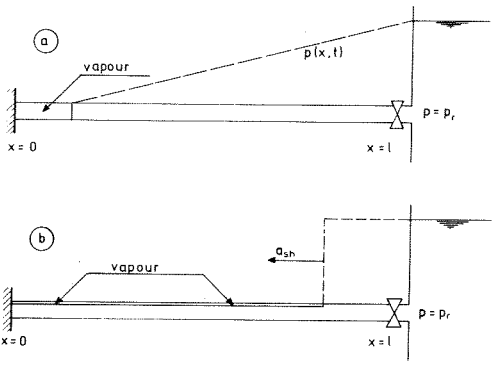

Fig. A2. Pipe containing void, a. Local cavity, b. distributed cavity.

For the sake of convenience the elasticity of the liquid and the pipe wall is disregarded ($a_l \to \infty$) as long as vapour is present in the pipe. The vapour pressure and vapour density are put equal to zero; the volume, V_v, of vapour is relatively small ($V_v << V_l$). No free gas is present. The two cases are discussed briefly.

Case a.

Rigid-column theory gives

$$p_r A \simeq - \rho A_l \frac{du}{dt} = - \rho_l A l \frac{d^2 s}{dt^2}$$

Integrating yields, together with the initial conditions u(0) = 0, and s(0) = 0,

$$u = - \frac{p_r}{\rho_l l} t \qquad \text{and} \qquad s = - \frac{1}{2} \frac{p_r}{\rho_l l} t^2 = - \frac{1}{2} \frac{\rho_l l}{p_r} u^2$$

At the instant ($t = t_a$) of cavity closure, s is equal to $-V_v/A$, and

$$t_a = l \sqrt{2 \frac{V_v}{V_l} \frac{\rho_l}{p_r}}$$

$$u_a = u(t_a) = - \sqrt{2 \frac{V_v}{V_l} \frac{p_r}{\rho_l}}$$

The water-hammer pressure (p_a) following column separation is

$$p_a = \rho_l a_l |u_a|$$

Case b.

When the valve is opened a shock wave starts to propagate in negative x-direction. Since in this case $p_2 = p_r$, $p_1 = 0$, $u_1 = 0$ and

$$\rho_f = \begin{cases} \rho_l (1 - \frac{V_v}{V_l}), & p = 0 \\ \rho_l, & p > 0 \end{cases}$$

Eqs. A13 and A14 yield

$$W^*_{sh} = \frac{1}{2} \frac{V_v}{V_l} \frac{p_r}{\rho_l}$$

$$a_{sh} = \sqrt{\frac{V_l}{V_v} \frac{p_r}{\rho_l}}$$

$$u_b = -\left(\frac{1}{\sqrt{1 - V_v/V_l}} - \sqrt{1 - V_v/V_l}\right) \sqrt{\frac{V_l}{V_v} \frac{p_r}{\rho_l}} \simeq -\sqrt{\frac{V_v}{V_l} \frac{p_r}{\rho_l}}$$

in which $u_b = -u_2$ = liquid velocity behind the shock wave. The shock wave arrives at $x = 0$ at $t = t_b$,

$$t_b = \frac{l}{a_{sh}} = l \sqrt{\frac{V_v}{V_l} \frac{\rho_l}{p_r}}$$

At this moment the liquid velocity is equal to u_b in the whole pipe, while all voids have vanished. Consequently, a water-hammer pressure

$$p_b = \rho_l a_l |u_b|$$

results.

Since $|u_b|$ is found to be equal to $|u_a|/\sqrt{2}$, the water-hammer pressure in case b is also lower by a factor $\sqrt{2}$. Also the duration of cavitation in case b is shorter

by this factor ($t_b = t_a/\sqrt{2}$).
The total energy loss in case b is

$$(V_l - V_v)\,\rho_l\,W^*_{sh} \simeq \frac{1}{2}\,V_v\,p_r$$

In both cases the work done during cavitation at x = l is equal to $V_v p_r$. This means that the energy loss must be equal to the difference in kinetic energies at the moment cavitation ceases to exist. This difference is

$$\frac{1}{2}\rho_l\,u_a^2\,V_l - \frac{1}{2}\rho_l\,u_b^2\,V_l = \frac{1}{2}(u_a^2 - u_b^2)\rho_l\,V_l$$

Substituting the obtained results for u_a and u_b shows this to be true indeed.

After the first pressure peak, in both cases column separation occurs at x = 0; the situation with distributed voids does not repeat itself spontaneously.

Fig. A3 presents a diagram of the pressure courses at x = 0 in cases a and b.

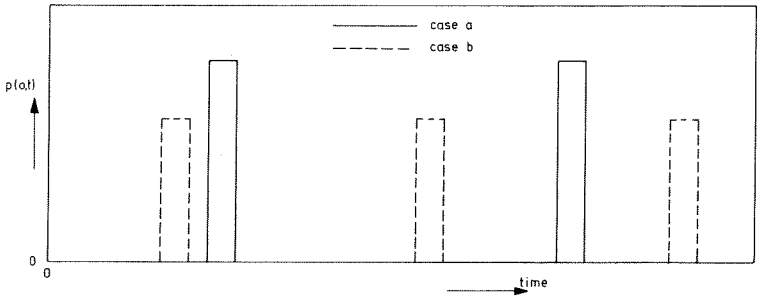

Fig. A3. Pressures at the closed end in cases a and b.

REFERENCES

1. Baltzer, R.A., "Column Separation Accompanying Liquid Transients in Pipes," Transactions of the ASME, Journal of Basic Engineering, Vol. 89, 1967, pp. 837-846.

2. Boussinesq, J., "Calcul du Pouvoir Refroidissant des Courants Fluides," Journal de Mathématiques Pures et Appliquées, Paris, Vol. 6, No. 1, 1905, pp. 285-332.

3. Brown, R.J., "Water-Column Separation at Two Pumping Plants," Transactions of the ASME, Journal of Basic Engineering, Vol. 90, 1968, pp. 521-531.

4. Campbell, I.J., and Pitcher, A.S.," Shock Waves in a Liquid Containing Gas Bubbles," Proceedings Royal Society, Series A, Vol. 243, 1958, pp. 534-545.

5. Dijkman, H.K.M., and Vreugenhil, C.B., "The Effect of Dissolved Gas on Cavitation in Horizontal Pipelines," Journal of Hydraulic Research, Vol. 7, No. 2, Nov., 1969, pp. 301-314.

6. Hsieh, D.-Y., and Plesset, M.S., "On the Propagation of Sound in a Liquid Containing Gas Bubbles," The Physics of Fluids, Vol. 4, No. 8, Aug., 1961, pp. 970-975.

7. Kalkwijk, J.P.Th., and Kranenburg, C., "Cavitation in Horizontal Pipelines Due to Water Hammer," Journal of the Hydraulics Division, ASCE, Vol. 97, No. HY10, Oct., 1971, pp. 1585-1605.

8. Kalkwijk, J.P.Th., and Kranenburg, C., "Cavitation in Horizontal Pipelines Due to Water Hammer," Report No. B/71/3, Laboratory of Fluid Mechanics, Dept. of Civil Engineering, Delft University of Technology, Delft, The Netherlands, 1971.

9. Knapp, R.T., Daily, J.W., and Hammitt, F.G., Cavitation, McGraw-Hill Book Co., New York, 1970.

10. Kranenburg, C., "The effects of Free Gas on Cavitation in Pipelines," Proceedings of the 1st International Conference on Pressure Surges. British Hydromechanics Research Association, 1972, pp. (C4)41-52.

11. Kranenburg, C., "Transient Cavitation in Pipelines," Report No. 73-2, Laboratory of Fluid Mechanics, Dept. of Civil Engineering, Delft University of Technology, Delft, The Netherlands, 1973.

12. Richtmeyer, R.D., and Morton, K.W., Difference Methods for Initial Value Problems, Interscience Publ., New York, 1967.

13. Streeter, V.L., and Wylie, E.B., Hydraulic Transients, McGraw-Hill Book Co., New York, 1967.

14. Streeter, V.L., "Transients in Pipelines Carrying Liquids or Gases," Transportation Engineering Journal, ASCE, Vol. 97, No. TE1, Feb., 1971, pp. 15-29.

15. Swaffield, J.A., "A Study of the Influence of Air Release on Column Separation in an Aviation Kerosine Pipeline," Proceedings of the Institution of Mechanical Engineers, Thermodynamics and Fluid Mechanics Group, Vol. 186, 1972, pp. 693-703.

16. Vliegenthart, A.C. "The Shumann Filtering Operator and the Numerical Computation of Shock Waves," Journal of Engineering Mathematics, Vol. 4, No. 4, 1970, pp. 341-348.

17. Vreugdenhil, C.B., et al., "Investigation into Cavitation in Long Horizontal Pipelines Caused by Water Hammer," Transactions of the Symposium of the Section for Hydraulic Machinery, Equipment and Cavitation, International Association for Hydraulic Research, Vol. 1, 1972, Paper No. J3, 13 p.

18. Weyler, M.E., Streeter, V.L., and Larsen, P.S., "An Investigation of the Effect of Cavitation Bubbles on the Momentum Loss in Transient Pipe Flow," Transactions of the ASME, Journal of Basic Engineering, Vol. 93, 1971, pp. 1-10.

NOTATION

A = area of cross-section of the pipe

a = wave celerity

B = constant in compatibility equation

D = diameter of the pipe

E = modulus of elasticity of the pipe wall material

F = function in gas-release relationship

g = gravitational constant

i,j = indices

K = modulus of compressibility

k = universal gas constant

l = length of the pipe

N = quantity of released gas

n = number of bubbles

P = production of mass

p = absolute pressure

Q = production of momentum

q_{ji} = variable in conservation law

$\overline{q}_{1i}$ = smoothened variable

R = bubble radius

T = absolute temperature

s = displacement

t = time variable

U = bubble velocity with respect to the surrounding liquid

u = liquid velocity

v = liquid velocity with respect to shock wave

V = volume

w = thickness of the wall of the pipe

W = work or energy

W^* = energy loss per unit mass

x = coordinate along the axis of the pipeline

α = local void-fraction

$\overline{\alpha}$ = cross-section averaged void-fraction

β = diffusion coefficient

γ = proportionality constant in Henry's law

Δ = increase of a variable across a shock wave

$\Delta x, \Delta t$ = mesh size, time step

θ_i = parameter in smoothening operator

λ = friction parameter

μ = free-gas content = $n_b N_b kT/A$

ρ = density

τ = dummy variable, wall shear stress

ϕ = angle of inclination of the pipeline

Subscripts

b = bubble

c = column separation

f = fluid

l = liquid

r = reference value, reservoir pressure

s = saturation (dissolved gas)

sh = shock wave

v = vapour